JOURNAL OF COMPUTATIONAL PHYSICS 111, 275–281 (1993)

High-Precision Calculations of Vortex Sheet Motion

JEFFREY S. ELY

Department of Mathematical Sciences, Lewis and Clark College, Portland, Oregon 97219

AND

GREGORY R. BAKER

Department of Mathematics, Ohio State University, Columbus, Ohio 43210

Received November 24, 1992; revised September 24, 1993

The motion of a vortex sheet undergoing Kelvin–Helmholtz instability is known to be ill-posed, causing deterioration in numerical calculations from the rapid growth of round-off errors. In particular, it is the smallest scales (introduced by round-off) that grow the fastest. Krasny ([12]) introduced a spectral filter to suppress the growth of round-off errors of the smallest scales. He was then able to detect evidence supporting asymptotic studies that indicate the formation of a curvature singularity in finite time. We use high precision interval arithmetic, coded in C++, to re-examine the evolution of a vortex sheet from initial conditions used previously by several researchers. Most importantly, our results are free from the influence of round-off errors. We show excellent agreement between results obtained through high precision interval arithmetic and through the use of Krasny's spectral filter. In particular, our results support the formation of a curvature singularity in finite time. After the time of singularity formation, the markers move in peculiar patterns. We rule out any possibility of this motion resulting from round-off errors, but it does depend on the level of resolution. We find no consistent behavior in the motion of the markers as we improve the resolution of the vortex sheet. Also, we find some disagreement between the results obtained through high precision interval arithmetic and through the use of the spectral filter.

1. INTRODUCTION

Vortex sheets arise frequently as models for thin shear layers or sharp interfaces between inviscid liquids. They are defined as surfaces (curves in two-dimensional flow) across which the fluid velocity, $\mathbf{u}$, has a jump discontinuity in its tangential component. Mathematically, a vortex sheet can be regarded as a delta function, defined on a surface, of the vorticity $\boldsymbol{\omega} = \nabla \times \mathbf{u}$. Some examples of studies of free-surface flows based on vortex sheets include Rayleigh–Taylor instabilities [3, 20, 26, 29, 2]; the motion of bubbles or drops [5, 28, 13, 9]; and the motion of water waves and internal waves [4, 20, 21]. Evidence from these calculations, in particular [2, 9], shows that curvature singularities form in finite time unless one side of the interface is a vacuum.

The underlying mechanism for singularity formation is believed to be the Kelvin–Helmholtz instability [10]. As the interface moves, regions form where the liquids flow with different speeds on either side of the interface. These regions appear on a small enough scale to be vortex sheets with almost uniform strength. These regions then suffer from the rapid development of the Kelvin–Helmholtz instability, where disturbances of the smallest length grow the fastest. Such behavior is a typical manifestation of ill-posed behavior.

The two-dimensional, periodic motion of a vortex sheet is governed by the periodic form of the Birkhoff–Rott equation,

$$\frac{\partial z^*}{\partial t}(p, t) = \frac{1}{4\pi i}\,\text{P.V.}\int_0^{2\pi} \mu(q)\cot\frac{z(p, t) - z(q, t)}{2}\,dq, \quad (1)$$

where $z(p, t) = x(p, t) + iy(p, t)$ gives the location of the sheet at time t. We assume the parametrization for the interface satisfies, $z(p + 2\pi, t) = 2\pi + z(p, t)$. The un-normalized vortex sheet strength $\mu(p)$ is a constant in time. The superscript * implies complex conjugation, and the integral is taken as a principal value.

Normally, studies of Kelvin–Helmholtz instability consider the evolution of periodic disturbances to a flat sheet, $z = p$, of uniform vortex sheet strength, $\mu = 1$. Asymptotic studies [15, 17, 7] have presented an interesting mathematical picture of how singularities form on vortex sheets. The analytic extension of $x(p, t)$, $y(p, t)$ to the complex p plane shows the presence of branch point singularities away from the real axis of p. In time, these singularities move

0021-9991/94 $6.00

towards the real axis of p and reach it in finite time. At this moment, a singularity in curvature becomes physically apparent. Recently, there has been much interest in confirming the asymptotic results by direct numerical solution of (1).

Ever since the first calculations by Rosenhead [22], various numerical methods have been applied to (1). Usually a simple, standard quadrature rule is applied to the integral and collocation is used to obtain a system of ordinary differential equations for discrete markers on the interface. Rosenhead introduced the approximation, based on the trapezoidal rule,

$$\frac{dz^*}{dt}(t)=\frac{1}{2Ni}\sum_{k\neq j}^{N}\mu_k\cot\frac{z_j-z_k}{2} \tag{2}$$

that has become known as the point vortex method. Here $z_j=x(jh)+iy(jh)$ and $\mu_j=\mu(jh)$, where $Nh=2\pi$. Unfortunately, numerical results always run into difficulties with the rapid development of the smallest scales available in the discretization [23]. Much of the early debate centered on whether truncation errors or round-off errors produce the irregular motion [6, 8, 27, 16]. The truncation error for the point vortex method is only $O(h)$ because of the poor numerical approximation to a principal-valued integral.

Krasny [12] made much progress in addressing these issues by using different levels of precision in his numerical calculations and showing clearly that the irregular motion of the markers is reduced with increasing precision. Even by using the highest precision available on standard computers, results still show the effects of round-off when using the large number of markers necessary to understand singularity development. Instead, Krasny introduced a spectral filter: the Fourier coefficients of $x(p, t)$, $y(p, t)$ are determined by using the fast Fourier transform, and all the coefficients below a certain filter level are set to zero. A new profile is reconstituted by the inverse fast Fourier transform. Without the filter, the Fourier spectrum of the initial data decays until the coefficients contain only round-off values. Because of the mathematical properties of the motion, the round-off values in the very highest wave-numbers grow the fastest, so that the profile soon becomes irregular. By selecting an appropriate filter level, these coefficients remain zero until nonlinear effects in the equation produce values above the filter level. Krasny's results show convergence with improvement in resolution up until a critical time, t_s. Detailed examination of the Fourier spectrum shows consistency with the interpretation that complex singularities in the p plane are approaching the real axis and reaching it at a time close to (if not equal to) t_s. The numerical results do not converge after t_s, and there is a difficult mathematical question on the nature of the vortex sheet after singularity formation.

Subsequently, Shelley [24] used a spectrally accurate method [25] for the Birkhoff–Rott integral (1),

$$\frac{dz_j^*}{dt}(t)=\frac{1}{iN}\sum_{\substack{k=0\\(k+j)\text{ odd}}}^{N}\mu_k\cot\frac{z_j(t)-z_k(t)}{2}, \tag{3}$$

together with the spectral filter to control round-off errors. He examined the influence of the filter level and found that very low filter levels are needed to obtain good accuracy in studying the behavior of the singularities in the complex p plane. Other work [19] also describes the influence of the filter level. While the results presented in these numerical studies involving spectral filters is persuasive, there is still the possibility that the filter acts in a subtle way to change the Fourier spectrum and so change the numerical solution. In this paper, we shall show convincingly that this is not the case.

While the main thrust of our study is to check the reliability of the spectral filter, the use of non-interval, high precision, floating point computations may be a practical option for vortex sheet motion without spatial periodicity. For example, we mention the MPFUN package of D. H. Bailey at NASA Ames, which provides a translator for standard Fortran to high precision code. Such an approach does not bound the round-off errors but may be somewhat faster than the use of intervals.

2. HIGH PRECISION INTERVAL ARITHMETIC

We apply high precision interval arithmetic to solve (3) with initial condition $z_j=jh$ and with $\mu_j=1+a\cos(jh)$. Our choice is motivated by the desire to compare with the results of Shelley [24].

Interval arithmetic [18] was introduced originally as a way to track bounds on the influence of finite precision rigorously. Numbers are represented by intervals, and arithmetic operations produce new intervals inside of which the actual result must lie. Unfortunately, for ill-posed problems the intervals soon become too wide for any useful information when the standard precision available on computers is used. Instead, we employ interval arithmetic, coded especially in high precision, so that we can guarantee the level of accuracy in the results even for late times of the solution to (3). Consequently, we can clearly separate the influence of the errors associated with round-off and with discretization.

Of course, our results will still suffer from truncation errors. Since the spatial discretization of the integral is spectrally accurate (at least before the singularity time), the truncation error is dominated by the method used to advance the solution in time. We employ several different methods; simple Euler, Runge–Kutta, Adams–Moulton, and Taylor series. Unfortunately, the cost of using high

precision interval arithmetic on this problem is high, so we are limited in the resolution we can use. Nevertheless, we believe we obtain sufficient accuracy to confirm the reliability of the spectral filter, which is far more economical to use.

As a start, we merely guess the precision needed in the initial data. If the precision is inadequate, the intervals containing the exact result will grow too wide too quickly. By requesting more precision in the initial data and re-running the calculation, we will obtain much narrower intervals for a longer period of time. Of course, we pay an additional cost in computer time to obtain the more accurate results. The importance of intervals, as opposed to merely higher precision floating point numbers, is that with a wide interval, we *know* the answer is not very good and can then decide if we want to pay the price for a more accurate answer. Likewise, if we do choose higher precision, and if all intervals are narrow enough, we *know* the results are essentially free of round-off errors. This is precisely the tool needed to rule out round-off effects in the numerical solution of the Birkhoff–Rott equation (1).

For our first calculation, we use 128 bits of mantissa with $N=40$ and a time-step of $\Delta t=0.15$. The code runs for nearly 7 days on a 68030 processor and terminates because an interval becomes so wide that it allows a possible divide by zero. If we are to have any hope of calculating with a finer grid, some computational speedup must be discovered. Fortunately, the symmetry, $z(\pi+p,t)=2\pi-z(\pi-p,t)$, allows us to halve the range of integration and, more importantly, allows us to rewrite (1) as

$$\frac{\partial z^*}{\partial t}(p,t)=\frac{\sin z(p,t)}{2\pi i}\,\text{P.V.}\int_0^\pi \frac{1+a\cos(q)}{\cos z(q,t)-\cos z(p,t)}\,dq \tag{4}$$

(see (14) in the Appendix for a derivation of the result). In this form we need only $O(N)$ evaluations of cos and sin at each time level (although the entire algorithm still requires $O(N^2)$ operations), whereas direct use of the original form requires $O(N^2)$ trigonometric evaluations. Since high precision, trigonometric interval calculations are very expensive, this is a major improvement. We test the new approach with $N=10$ against the results of the previous approach with $N=20$ and find complete agreement.

In Fig. 1 we show the results of applying the fourth-order Adams–Moulton predictor–corrector with time-step 0.09375 and $N=64$ markers; we use 448 bits of mantissa and the calculation takes about 14 h on a 68030 processor. Beyond the time $t=1.6875$, a peculiar pattern in the markers soon sets in. Because we can bound the influence of round-off in these calculations (the widest interval $<10^{-20}$), we know this peculiarity is not caused by round-off errors.

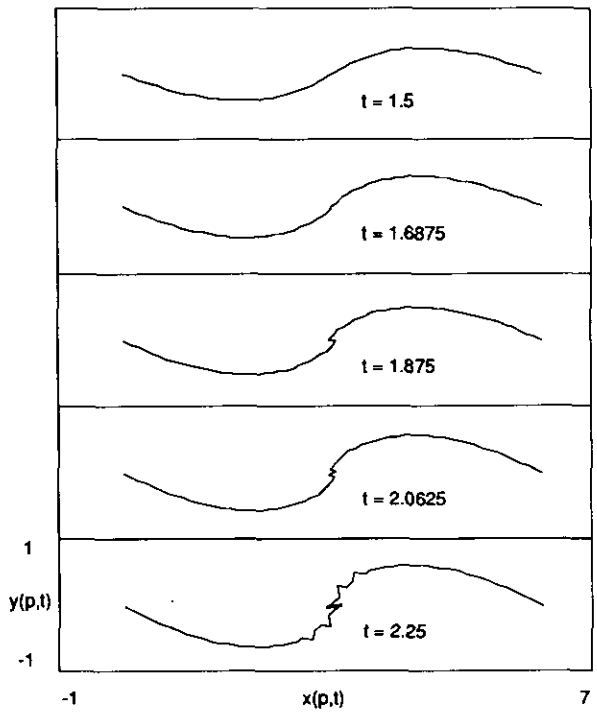

FIG. 1. A sequence of profiles showing the position of the vortex sheet in a periodic window as time increases. Results are shown from top to bottom at times: 1.5, 1.6875, 1.875, 2.0625, 2.25. Results are obtained with $\Delta t=9.375\times10^{-2}$, $N=64$, and 448 bits of mantissa.

To achieve our finest levels of resolution, we introduce a further simplification by defining $h(p,t)=\cos(z(p,t))$. We then transform (4) into

$$\frac{\partial h^*}{\partial t}(p,t)=\frac{|1-h^2(p,t)|}{2\pi i}\,\text{P.V.}\int_0^\pi \frac{\mu(q)}{h(p,t)-h(q,t)}\,dq. \tag{5}$$

Details are given in the Appendix. With this form we eliminate all trigonometric calculations except the determination of the initial condition for h which requires $N/2$ evaluations of $\cos(q)$. Of course, we will still have to invert the trigonometric mapping to graph the results, but this can be done in the usual low-precision, floating point format (specifically, the intrinsic C++ subroutines) as any round-off incurred in the single inversion per point is graphically unobservable. When we wish to study the Fourier coefficients at select time levels, we invert the trigonometric mapping in high precision interval arithmetic. Since we do this only occasionally, the cost is not excessive.

In Fig. 2 we show the results of just such a trig-free calculation. We use the fourth-order Adams–Moulton predictor–corrector with a time-step of 5.859375×10^{-3} and $N=128$. The results are obtained using 1152 bits of mantissa and require more than 3 days of processing. The widest interval during the calculation has width $<10^{-90}$, so we are certain that round-off errors are negligible in our results.

We show the results in Figs. 1 and 2 at the same times to

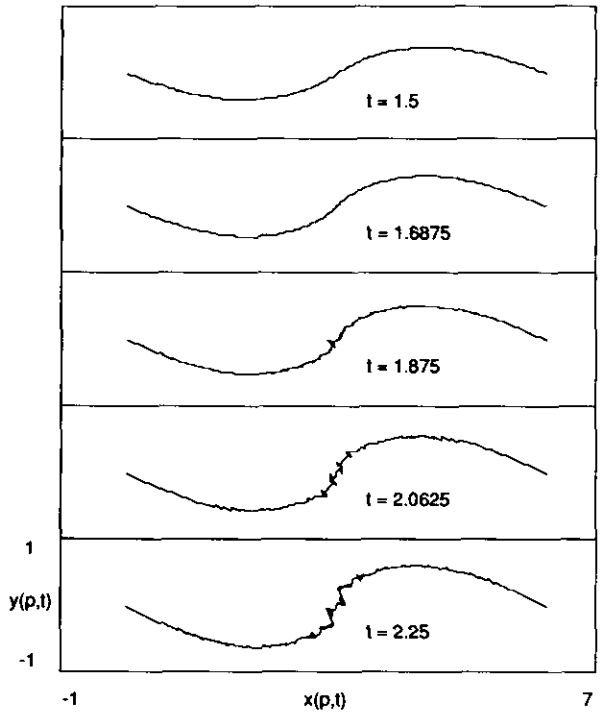

FIG. 2. A sequence of profiles showing the position of the vortex sheet in a periodic window as time increases. Results are shown from top to bottom at times: 1.5, 1.6875, 1.875, 2.0625, 2.25. Results are obtained with $\Delta t = 5.859375 \times 10^{-3}$, $N = 128$, and 1152 bits of mantissa.

highlight the influence of resolution especially at times around and beyond the singularity time $t_s = 1.615$. At times well beyond t_s, improvement in resolution does not give a smoother curve; in fact, the markers are even more erratic. Since truncation errors are the only significant errors in our results, we conclude that solutions to the discrete equation (3) will not converge to a smooth curve after the singularity time in the limit of infinite resolution. One possibility is that there is no smooth solution to (1) after the singularity time. Another possibility is that the solution undergoes a topological change which is no longer well resolved by our numerical approximation. For example, current speculation is that at $t = t_s$, the curvature singularity is immediately replaced by an infinitely small doubly branched spiral that subsequently grows in size.

3. FOURIER ANALYSIS

According to asymptotic predictions [15, 17, 7], a complex conjugate pair of branch point singularities in the complex p plane will move towards the real axis and reach it in finite time. If the branch points of power $\beta - 1$ are located at $p_s = (2m+1)\pi \pm i\alpha$, then the coefficients $A_k(t)$ of the Fourier representation,

$$z(p, t) = p + \sum_{k=-\infty}^{\infty} A_k(t)\, e^{ikp}, \tag{6}$$

will have the behavior for large k,

$$|A_k(t)| \sim Ck^{-\beta} e^{-\alpha(t)k}. \tag{7}$$

This behavior is true also for the real and imaginary parts of $z(p, t)$, and in practice, the Fourier coefficients of the numerical results for $x(p, t)$ and $y(p, t)$ are compared to the form (7). The fact that the singularities lie along lines at odd multiples of π is a consequence of our choice of initial condition. In previous work, the Fourier spectra of the numerical results are compared with (7) by a least squares fit over a suitable range in k [12]; the agreement is reasonably good.

An alternative approach is introduced by Pugh [19] to study singularity formation on interfaces in Boussines flows and applied by Shelley [24] to the Kelvin–Helmholtz instability. A local fit of data poins at $k-1$, k, $k+1$ is used to determine $\alpha_x(k, t)$, $\beta_x(k, t)$, $C_x(k, t)$, and $\alpha_y(k, t)$, $\beta_y(k, t)$, $C_y(k, t)$, where the subscripts x or y indicate whether $x(p, t)$ or $y(p, t)$, respectively, is used to obtain the coefficients. The coefficients can be easily determined from the equations,

$$\ln |A_m(t)| = \ln C - \beta \ln m - \alpha m, \quad \text{for} \quad m = k-1, k, k+1. \tag{8}$$

At a fixed time t, the behavior of the locally fitted coefficients can be studied for large k. If the asymptotic predictions are correct, then these coefficients should tend to constant values for large enough k. Shelley [24] uses this approach to confirm Krasny's [12] results and to study the influence of the spectral filter. He finds that by reducing the filter level, the results of the form fit settle down to a behavior that is determined by the resolution of the calculation. Over an intermediate range of k, the coefficients asymptote to constant values. For k near $N/2$, there is divergence from these constant values, reflecting the influence of truncation errors. Because Shelley uses a spectral method, the truncation effects are limited to values of k near $N/2$. Shelley introduces a correction to (8) that gives improved estimates for the coefficients. Since we are mainly concerned with the influence of the spectral filter, we repeat Shelley's calculations, but in high precision interval arithmetic. We fit our numerical results to (7) by means of (8) and compare our values for the coefficients with those obtained through use of the spectral filter.

In Fig. 3, we show the results of the form-fit at time $t = 1.5$. Our results are obtained from calculations of (5) with $N = 128$ by using high precision interval arithmetic. We vary the time-steps in the fourth-order Adams–Moulton predictor–corrector to check the accuracy of the resolution. In the first three columns, we show the improvement in the results as the time-step decreases from $\Delta t = 4.6875 \times 10^{-2}$ to $\Delta t = 2.9296875 \times 10^{-3}$. In the final column, we give the results from using a spectral filter at a level $\delta = 10^{-25}$ applied to the solution of (3). Following Shelley, we use the

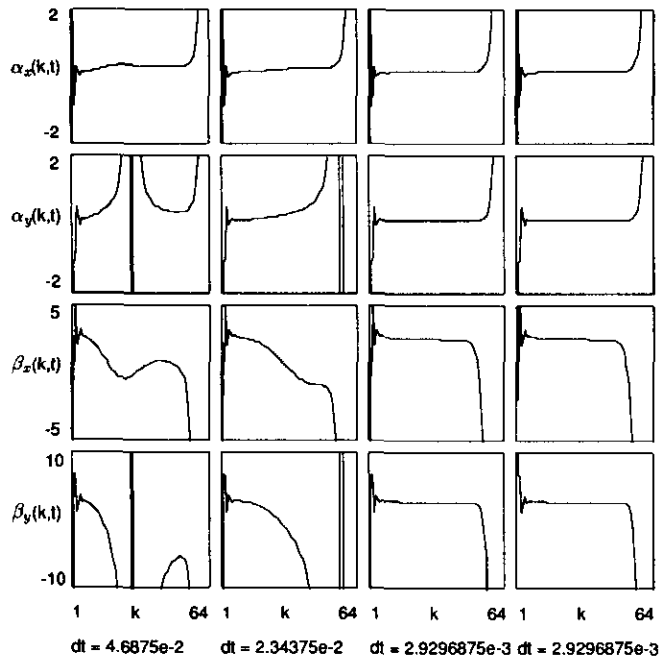

FIG. 3. The coefficients, α and β, determined locally for the form fit (7) and obtained from high precision interval arithmetic with different step-sizes. Columns 1–3 correspond to $\Delta t = 4.6875 \times 10^{-2}$, 2.34375×10^{-2}, 2.9296875×10^{-3}, respectively. The last column gives the results from application of a spectral filter with $\Delta t = 2.9296875 \times 10^{-3}$. All columns are snapshots at time 1.5.

fourth-order Adams–Moulton predictor–corrector and run our code in double precision on a CRAY Y-MP/64. We use $N = 128$ and a time-step $\Delta t = 2.9296875 \times 10^{-3}$ to be able to make a direct comparison with the results in column 3.

We show the results only for the physically important coefficients α and β in the fit to the Fourier coefficients of $x(p, t)$ and $y(p, t)$. Similar results are obtained for the coefficient C. A comparison of the results in columns 3 and 4 show excellent agreement between calculations based on high precision interval arithmetic and on the spectral filter. In fact, the position of the markers agree to 10 digits except very near to $p = \pi$, where the agreement is eight digits. There is a 3–4 digit agreement in the values of α and β. Although we show only one such comparison, the result is typical for times before the singularity formation, $t_s = 1.615 \pm 0.01$. Incidentally, the fact that the values of α and β diverge abruptly near $k = 64$ from their nearly constant values is associated with the spatial resolution. Shelley shows that increases in N extend the range for which α and β remain close to constants.

Next we consider what happens to the form fit as time approaches and passes t_s. In Figs. 4 and 5, we show α and β obtained through calculations in high precision interval arithmetic and through application of a spectral filter, respectively. These results have the same resolution as those in column 3 and 4 in Fig. 3. Note how the coefficient α

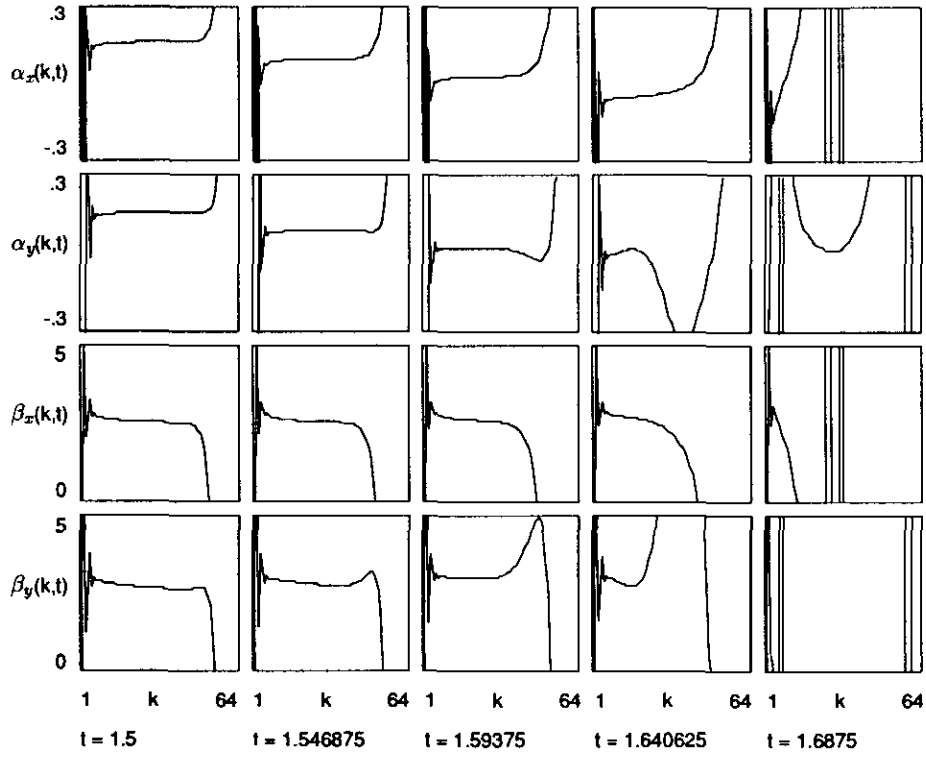

FIG. 4. The behavior of the coefficients, α and β, determined locally for the form fit (7) and obtained from high precision interval arithmetic for various times: 1.5, 1.546875, 1.59375, 1.640625, 1.6875 with $\Delta t = 2.9296875 \times 10^{-3}$.

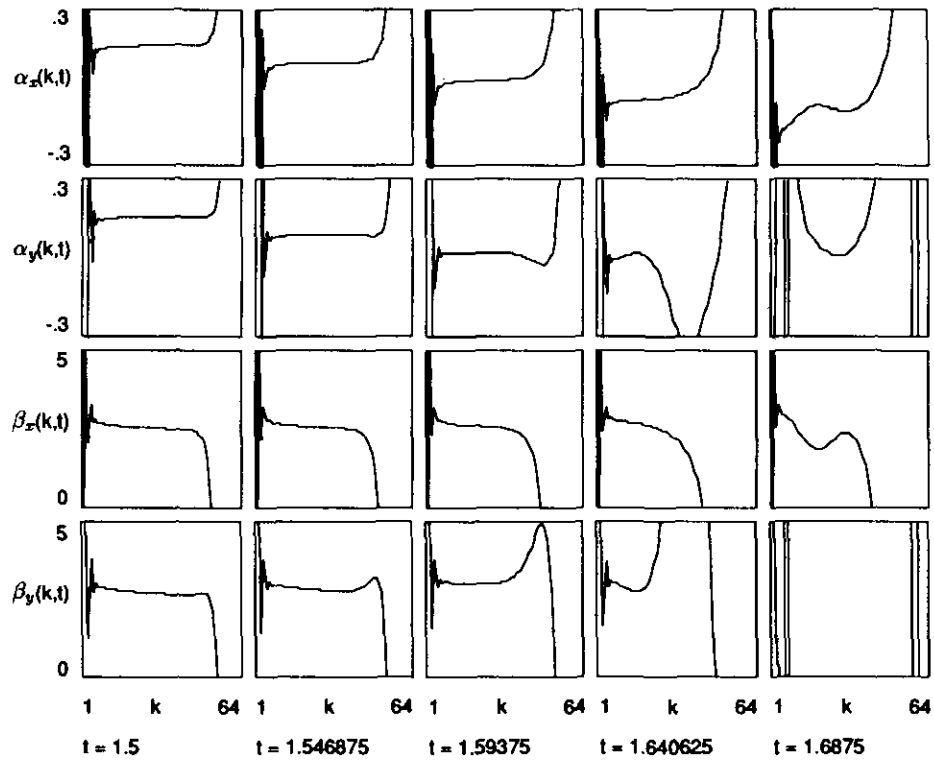

FIG. 5. The behavior of the coefficients, α and β, determined locally for the form fit (7) and obtained from use of a spectral filter for various times: 1.5, 1.546875, 1.59375, 1.640625, 1.6875 with $\Delta t = 2.9296875 \times 10^{-3}$.

passes through zero between $t = 1.59375$ and 1.640625. Since Shelley has discussed fully the implications of these results, we include a brief summary for the interested reader. By extrapolating the change of α in time, Shelley obtains the estimate, $t_s = 1.615 \pm 0.01$. At that moment, the convergence of the Fourier series is dictated by the algebraic decay in the coefficients. Shelley shows that $\beta \approx 2.5$ by including more terms in the asymptotic behavior (7), although he does detect $\beta_y > \beta_x$ ($\beta_y \approx 3$) for large initial amplitudes. In either case, the second derivative of $z(p, t_s)$ blows up, indicating the presence of a curvature singularity. For times just beyond t_s, α appears negative, and the Fourier series does not converge.

In this paper, our main interest is in examining the possible influence of the spectral filter. We note that even up to $t = 1.640625$, just after singularity formation, there is excellent agreement between both methods. However, at $t = 1.6875$, there are clear differences between the coefficients of the form fit to the Fourier coefficients of $x(p, t)$. It is important to recognize that when α is small, that is, just before t_s, the decay of the Fourier spectra is so slow that all amplitudes up to $k = 64$ lie above the filter level, so that in effect the filter is turned off. Consequently, the differences in data at $t = 1.6875$ reflect the presence of very small differences in the data before t_s. In this regard, the filter does have an important influence on the results. There remains much current interest in the nature of the vortex sheet beyond t_s.

4. CONCLUSIONS

Calculations with high precision interval arithmetic confirm that the motion of a vortex sheet is well defined up to the time of singularity formation. Beyond this time, the erratic motion of the markers is not caused by round-off errors. Application of the spectral filter of Krasny [12] also suppresses the growth of round-off errors with excellent agreement with results from high precision interval arithmetic. However, agreement is lost after the singularity time. The sensitivity of the motion of the markers to round-off errors or truncation errors after the time of singularity is clearly demonstrated.

APPENDIX

We take advantage of the symmetry in our problem to reduce (1) to a form more suitable for high precision calculations. We start with the equation

$$\frac{\partial z^*}{\partial t}(p, t) = \frac{1}{4\pi i} \text{P.V.} \int_0^{2\pi} (1 + a\cos(q)) \times \cot\left(\frac{z(p, t) - z(q, t)}{2}\right) dq \qquad (9)$$

and initial condition $z(p, 0) = p$. Consider the above integral from just π to 2π and make the substitution, $q = Q + \pi$. By using the symmetry

$$z(\pi + Q) = 2\pi - z(\pi - Q), \tag{10}$$

we obtain

$$\text{P.V.} \int_{Q=0}^{\pi} (1 - a \cos Q) \cot\left(\frac{z(p, t) + z(\pi - Q, t)}{2}\right) dQ. \tag{11}$$

We use another substitution, $q = \pi - Q$, to obtain

$$\text{P.V.} \int_0^{\pi} (1 + a \cos q) \cot\left(\frac{z(p, t) + z(q, t)}{2}\right) dq. \tag{12}$$

By adding (12) to the integral from 0 to π in (9) and by using the relation

$$\cot \alpha + \cot \beta = \frac{2 \sin(\alpha + \beta)}{\cos(\alpha - \beta) - \cos(\alpha + \beta)}, \tag{13}$$

we find

$$\frac{\partial z^*}{\partial t}(p, t) = \frac{\sin z(p, t)}{2\pi i} \text{P.V.} \int_0^{\pi} \frac{1 + a \cos q}{\cos z(q, t) - \cos z(p, t)} dq. \tag{14}$$

Now define $h(p, t) = \cos z(p, t)$, then $h^*(p, t) = \cos z^*(p, t)$ and

$$\begin{aligned} \frac{\partial h^*}{\partial t}(p, t) &= -\sin z^*(p, t) \frac{\partial z^*(p, t)}{\partial t} \\ &= -\frac{|\sin z(p, t)|^2}{2\pi i} \text{P.V.} \int_0^{\pi} \frac{1 + a \cos q}{\cos z(q, t) - \cos z(p, t)} dq \\ &= -\frac{|\sin^2 z(p, t)|}{2\pi i} \text{P.V.} \int_0^{\pi} \frac{1 + a \cos q}{\cos z(q, t) - \cos z(p, t)} dq \\ &= -\frac{|1 - h^2(p, t)|}{2\pi i} \text{P.V.} \int_0^{\pi} \frac{1 + A \cos q}{h(q, t) - h(p, t)} dq. \end{aligned} \tag{15}$$

Our initial condition becomes $h(p, 0) = \cos p$.

REFERENCES

1. G. R. Baker, "Generalized Vortex Methods for Free-Surface Flows," in *Waves on Fluid Interfaces*, edited by R. E. Meyer (Academic Press, New York, 1983), p. 53.
2. G. R. Baker, R. E. Caflisch, and M. Siegel, *J. Fluid Mech.* **252**, 51 (1993).
3. G. R. Baker, D. I. Meiron, and S. A. Orszag, *Phys. Fluids* **23**, 1485 (1980).
4. G. R. Baker, D. I. Meiron, and S. A. Orszag, *J. Fluid Mech.* **123**, 477 (1982).
5. G. R. Baker and D. W. Moore, *Phys. Fluids A* **1**, 1451 (1989).
6. G. Birkhoff, "Helmholtz and Taylor Instability," in *Proc. Symp. Appl. Math.*, Vol. XIII (Am. Math. Soc., Providence, RI, 1962), p. 55.
7. R. Caflisch, O. Orellana, and M. Siegel, A localized approximation method for vortical flows, *SIAM J. Appl. Math.* **50**, 1517 (1990).
8. A. J. Chorin and P. S. Bernard, *J. Comput. Phys.* **13**, 423 (1973).
9. S. Cowley and D. Pugh, *J. Fluid Mech.*, to appear.
10. P. G. Drazin and W. H. Reid, *Hydrodynamic Stability* (Cambridge Univ. Press, London, 1981).
11. H. Kagiwada, R. Kalaba, N. Rasakhoo, and K. Spingarn, *Numerical Derivatives and Nonlinear Analysis* (Plenum, New York, 1986).
12. R. Krasny, *J. Fluid Mech.* **167**, 65 (1986).
13. T. S. Lundgren and N. N. Mansour, *J. Fluid Mech.* **194**, 479 (1988).
14. D. Meiron, G. Baker, and S. Orszag, *J. Fluid Mech.* **114**, 283 (1982).
15. D. W. Moore, *Proc. R. Soc. London A* **365**, 105 (1979).
16. D. W. Moore, *SIAM J. Sci. Stat. Comput.* **2**, 65 (1981).
17. D. W. Moore, "Numerical and Analytical Aspects of Helmholtz Instability," in *Theoretical and Applied Mechanics*, edited by F. I. Niordson and N. Olhoff (Elsevier, New York, 1985).
18. R. Moore, *Methods and Applications of Interval Analysis* (SIAM, Philadelphia, 1979).
19. D. Pugh, "Development of vortex sheets in Boussinesq flows—Formation of singularities," Ph.D. thesis, Imperial College, University of London, 1989.
20. D. I. Pullin, *J. Fluid Mech.* **119**, 507 (1982).
21. A. J. Roberts, *IMA J. Appl. Math.* **31**, 13 (1983).
22. L. Rosenhead, *Proc. R. Soc. London A* **134**, 170 (1931).
23. P. G. Saffman and G. R. Baker, *Annu. Rev. Fluid Mech.* **11**, 95 (1979).
24. M. J. Shelley, *J. Fluid Mech.* **244**, 493 (1993).
25. A. Sidi and M. Israeli, *J. Sci. Comput.* **3**, 201 (1988).
26. G. Tryggvason, *J. Comput. Phys.* **75**, 253 (1988).
27. A. I. Van de Vooren, *Proc. R. Soc. London A* **373**, 67 (1980).
28. Y. Yang, *Phys. Fluids A* **4**, 913 (1992).
29. J. A. Zufiria, *Phys. Fluids* **31**, 3199 (1988).